Analysis and Compensation for HPA Nonlinearity with Neural Network in MIMO-STBC Systems

Oussama B. Belkacem†, Mohamed L. Ammari†, Rafik Zayani† and Ridha Bouallegue†
belkacemoussema@supcom.rnu.tn mlammari@ele.etsmtl.ca rafik.zayani@supcom.rnu.tn ridha.bouallegue@supcom.rnu.tn
†SUPCOM, Innov'Com Laboratory, Carthage University, Tunis, Tunisia

***Abstract*—In order to provide high data rate over wireless channels and improve the system capacity, Multiple-Input Multiple-Output (MIMO) wireless communication systems exploit spatial diversity by using multiple transmit and receive antennas. Moreover, MIMO systems are equipped with High Power Amplifiers (HPA). However, HPA causes nonlinear distortions and affect the receiver's performance. Since a few decades, Neural Networks (NN) have shown excellent performance in solving complex problems like classification, recognition and approximation. In this paper, we present a receiver technique based on NN schemes for the compensation of HPA non linearization in MIMO Space-Time Block Coding (STBC) systems. Specifically, we assess the impact of HPA nonlinearity and NN on the average symbol error rate (SER) and the error vector magnitude (EVM) of MIMO-STBC in uncorrelated Rayleigh fading channels. Computer simulation results confirm the accuracy and validity of our proposed analytical approach.**

***Index Terms*—MIMO(Multiple Input Multiple Output), HPA(High Power Amplifier), NN(Neural Network), SER(Symbol Error Rate), EVM(Error Vector Magnitude).**

I. Introduction

Wireless services are driven by the rising demand to provide high-speed data transmissions (several 100 Mbit/s). A common way to improve the system capacity is to increase the transmission bandwidth. Multiple-Input Multiple-Output (MIMO) has been proposed to develop wireless systems that offer both high capacity and better performance. It has been recognized as a key technology for 4G wireless communications [1], [2].

High-power amplifier (HPA) is a primary block of a wireless communication system, such us Travelling Wave Tube Amplifier (TWTA), Solid State Power Amplifier (SSPA) and Soft-Envelope Limiter (SEL). It operates between the modulator and radio frequency (RF) modules. However, HPA introduces nonlinear distortions to the transmitted signal when operating in nonlinear region [3]. Nonlinear distortions, including amplitude and phase distortions, are introduced into the transmitted symbols, which in turn can cause adjacent channel interference and power loss. These distortions degrade considerably the system performance.

Nonlinear HPA can be described by two kinds of models: memoryless models with flat frequency responses, and memory models with frequency-selective responses [4]. Memoryless HPA models, such as the TWTA, SSPA and SEL, are characterized by their amplitude modulation/amplitude modulation (AM/AM) and amplitude modulation/phase modulation (AM/PM) conversions [5]. On the other hand, HPA may be characterized by more realistic memory models, such as the Volterra, Wiener, Hammerstein and memory polynomial models [3], [4].

To improve the system throughput, the effect of HPA was analyzed in [3] for MIMO systems employing Orthogonal Space Time Block Coding (OSTBC). In [1], authors proposed an adaptive predistortion technique based on a feed-forward Neural Network (NN) to linearize power amplifiers such as those used in satellite communications. Authors in [6] extended the efficient NN Predistorter (NNPD) to MIMO-OFDM systems. In [7], NN technique has gained a great interest in nonlinear MIMO channel identification and authors proposed an efficient nonlinear receiver to compensate the joint effects of HPA nonlinearity and the impact of time-varying MIMO channels. In this paper, we focus on HPA nonlinearity on MIMO-STBC systems. we propose a NN compensator technique to enhance nonlinearity distortion at the receiver. For the outlined transmission chain, we derive the expressions for the average SER and EVM, which are valued for memoryless nonlinear HPA models, considering that the system operates under Rayleigh flat fading channel. The remainder of the paper is organized as follows: Section II

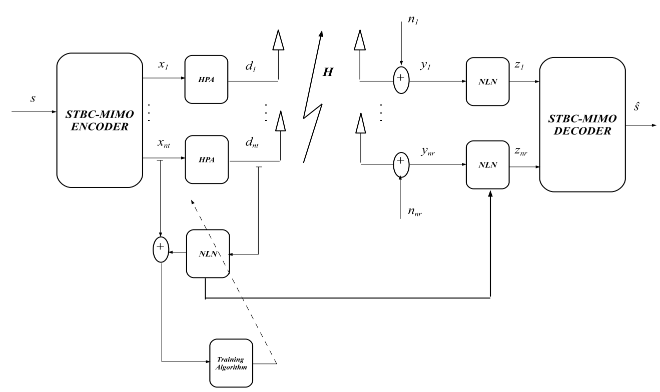

Fig. 1. Block diagram of the considered MIMO-STBC system in the presence of nonlinear HPA and NLN compensation.

introduces the MIMO system model with HPA nonlinearity, the NN scheme is revisited and explained. In Section III, we derive the exact SNR expression in presence of NN compensation scheme and evaluate the system performance in terms of SER and EVM in the case when knowledge

 ISBN: 978-1-61208-236-3

of the HPA parameters is available. Numerical results and comparisons are then presented in Section IV. We complete this study by conclusions in Section V.

II. System Model

A. MIMO-STBC and HPA nonlinearity

The block diagram of the considered MIMO-STBC system is shown in Figure 1. The MIMO-STBC system is equipped with n_t transmit and n_r receive antennas. In frequency non-selective block-fading channels, assuming that the x_l are M-QAM modulated symbols of period $\boldsymbol{T}$ and average energy $\boldsymbol{P}_s$ for $l = 1, \cdots, n_t$. the received signal is given by

$$\boldsymbol{Y} = \boldsymbol{H}\boldsymbol{D} + \boldsymbol{N} \tag{1}$$

where $\boldsymbol{Y} \in \mathcal{C}^{n_r \times \boldsymbol{T}}$ is the received matrix, $\mathbf{H} = [h_{k,l}]^{n_r,n_t} \in \mathcal{C}^{n_r \times n_t}$ indicates the $n_r \times n_t$ channel gain matrix with $h_{k,l}$ representing the channel coefficient between the lth transmit and the kth receive antennas and $\mathbf{N}$ is the Additive White Gaussian Noise (AWGN) matrix with *i.i.d.* entries $\sim \mathcal{CN}(0, N_0)$.

The transmitted signal $\boldsymbol{D} \in \mathcal{C}^{n_t \times \boldsymbol{T}}$ has to be amplified at RF through the HPA, which may operate in its nonlinear region, causing amplitude distortion and phase distortion on the input signal [8]. We consider memoryless HPA that can be characterized by their AM/AM and AM/PM conversions. We denote the input signal at the HPA as

$$x_l = r_l e^{j\theta_l} \tag{2}$$

where $r_l(.)$ is the input modulus and $\theta_l(.)$ is the input phase. The signal at the output of the HPA can be expressed as

$$d_l = A_l\,(r_l) \exp\{P_l(r_l) + \theta_l\} \tag{3}$$

where $A_l(.)$ and $P_l(.)$ denote the HPA amplitude conversion (AM/AM) and phase conversion (AM/PM), respectively.

Many models are tailored for a particular type of HPA. TWTA and SSPA as in [9], and SEL as in [10]. The TWTA can be characterized by the Saleh's model [5], which has the advantage of exhibiting greater simplicity and accuracy than other models. The AM/AM and AM/PM conversions can be represented as follow

$$A(r_l) = \tfrac{\alpha_a r_l}{1+\beta_a r_l^2} \quad \text{and} \quad P(r_l) = \tfrac{\alpha_p r_l^2}{1+\beta_p r_l^2} \tag{4}$$

where α_a and β_a are the parameters of the non-linear level, and α_p and β_p are phase displacements. The AM/AM and AM/PM conversions of the SSPA model first and SEL model are the following

$$A(r_l) = \frac{r_l}{\left[1+\left(\frac{r_l}{A_{os}}\right)^{2\beta}\right]^{1/2\beta}} \quad \text{and} \quad P(r_l) = 0 \tag{5}$$

$$A(r_l) = \begin{cases} r_l & r_l \leq A_{is} \\ A_{is} & r_l > A_{is} \end{cases} \quad \text{and} \quad P(r_l) = 0 \tag{6}$$

where β indicates the flexibility of the transition from linear operation to saturation. A_{is} is the input saturation voltage and A_{os} is the output voltage at the saturation point. For simplicity, the HPAs at all the transmitting branches are assumed to exhibit the same nonlinear behavior [3], [11].

According to the central limit theorem, a signal can be approximated as a complex Gaussian distributed random process. From the Bussgang theorem and by extending that to complex Gaussian processes, the output signal at the HPA can be expressed as [12]

$$d_l = K_l x_l + w_l \tag{7}$$

where K_l denotes an arbitrary deterministic complex factor and w_l is a suitably additive zero-mean Gaussian noise uncorrelated with the input signal x_l. The value of K_l is given by [6, eq. (19)]

$$K_l = \frac{1}{2} E\left[d_l^{'}(r) + \frac{d_l(r)}{r}\right] \tag{8}$$

where $d_l^{'}(r)$ denotes the differential of $d_l(r)$. Furthermore, the variance of w_l is given by [12, eq. (37)]

$$\begin{aligned}\sigma_{w_l}^2 &= E[|w_l|^2] = E[|d_l|^2] - |K|^2 E[|x_l|^2] \\ &= E[A^2(r_l)] - |K|^2 E[r_l^2]\end{aligned} \tag{9}$$

Specifically, for the SEL model, the analytical evaluation of K_l and $\sigma_{w_l}^2$ values, can be obtained using [8] [6, eq. (42)] as follows

$$K_l = \left(1 - e^{-(A_{is}^2/\boldsymbol{P}_s)}\right) + \frac{1}{2}\sqrt{\pi \frac{A_{is}^2}{\boldsymbol{P}_s}} \text{erfc}\sqrt{\frac{A_{is}^2}{\boldsymbol{P}_s}} \tag{10}$$

$$\sigma_{w_l}^2 = \boldsymbol{P}_s \left(1 - e^{-(A_{is}^2/\boldsymbol{P}_s)} - K_l^2\right) \tag{11}$$

In addition, the parameters K_l and $\sigma_{w_l}^2$ for the TWTA and SSPA models has been evaluated in [12, Tab. I].

When the channel gain matrix is perfectly estimated at the receiver, the MIMO-STBC model can be converted into an equivalent single-input single-output (SISO) scalar model, yielding [3]

$$y = c\|\boldsymbol{H}\|_F^2 d + \tilde{n} \tag{12}$$

where $\|.\|_F$ denotes the Frobenius norm, d represents the distorted version of the transmitted symbol with average power $\boldsymbol{P}_s^{HPA} = K_l^2 \boldsymbol{P}_s$, c is a code-dependent constant based on the STBC mapping and $\tilde{n}$ is the noise term after STBC decoding with distribution $\sim \mathcal{CN}(0, c\|H\|_F^2 N_0)$. Consequently, the effective SNR at the output of the MRC decoder can be expressed as

$$\begin{aligned}\gamma^{STBC} &= \frac{c^2 K_l^2 \boldsymbol{P}_s \|\boldsymbol{H}\|_F^4}{\left(cN_0 + c\sigma_{w_l}^2\right)\|\boldsymbol{H}\|_F^2} \\ &= \frac{cK_l^2 \boldsymbol{P}_s}{N_0 + \sigma_{w_l}^2}\|\boldsymbol{H}\|_F^2 = \frac{c\boldsymbol{P}_s^{HPA}}{N_0 + \sigma_{w_l}^2}\|\boldsymbol{H}\|_F^2\end{aligned} \tag{13}$$

B. Architecture of the applied neural network

In our investigation, a multilayer perceptron is used to compensate the effect of HPA nonlinearity. A Nonlinear Network (NLN) (see Figure 2) is a very interesting model for adaptive equalisation due to its properties such as the parallel distributed architecture, the adaptive processing, the nonlinear approximation, the easy integration in large information processing chains and the efficient hardware implementation [13].

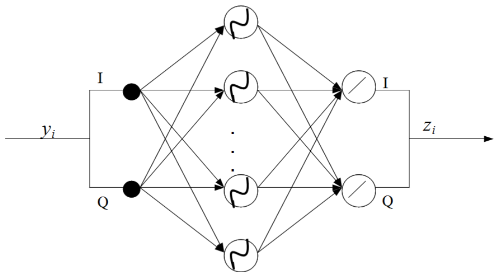

Fig. 2. A NLN multilayer perceptron neural network: This network has two layers, two input signals, one hidden layer, 2 neurons in the output layer, and 2 output signals. (Indexes I and Q refer to the real and imaginary parts, resp.)

Using the structure illustrated in Figure 1, we aim to identify the HPA inverse transfer functions. The complex envelope signals are differentiated and the error sent to the "learning algorithm" bloc reacts on coefficients of NLN. The weights of the NLN Receiver are determined by copying the weights of a trained network NLN.

The multilayer perceptron has two inputs, namely the I and Q components of the input signal complex envelope. The NLN has two outputs that are the compensated signals I and Q signals. Applying an input signal $\boldsymbol{y}_k = [\boldsymbol{y}_{k,I}, \boldsymbol{y}_{k,Q}]^t$, the output of the hidden neuron m [14]

$$v_{k,m} = f(\textstyle\sum_j w_{j,m} y_{k,j} + b_m) \tag{14}$$

where $w_{j,m}$ is the weight connection between $y_{k,j}$ and the neuron m for $(j = I, Q)$. The function f is a nonlinear activation function (hyperbolic tangent function). In this case, the output of the NLN can be expressed as

$$z_{k,j} = \textstyle\sum_m u_{m,j} v_{k,m} \tag{15}$$

where $u_{m,j}$ is the weight connecting the neuron m of the hidden layer to the neuron j of the output layer.

The received signal at the output of the neural network block may be modeled as the sum of the transmitted signal x_l and a noise factor caused by the effects of the NLN errors and the channel transmission. Consequently, the output signal $z_{k,j}$ can be approximated by

$$z_{k,j} \simeq x_{l,j} + \sum_m \hat{n}_{m,j} \tag{16}$$

where $\hat{n}_{m,j}$ is the noise of the m-th neuron of the hidden layer. Since f is not a linear activation function, $\hat{n}_{m,j}$ is a non gaussian random variable. However, using the central limit theorem, we can approximate $\sum_m \hat{n}_{m,j}$(the sum of 9 random variable in our case) as a gaussian noise.

During the training sequence, the NLN model uses supervised learning to update the weight parameters in order to minimize a cost function. This function is the sum of squared errors between the unknown system outputs and the HPA inputs (see Figure 2). For the training algorithm, we have chosen the Levenberg-Marquardt algorithm [1]. The contribution of this algorithm is similar to determinate the second-order training speed without having to compute the Hessian matrix. Under the assumption that the error function is some kind of squared sum, the Hessian matrix $\boldsymbol{He}$ can be approximated as

$$\boldsymbol{He} = \boldsymbol{J}^T \boldsymbol{J} \tag{17}$$

and the gradient can be computed as:

$$g = \boldsymbol{J}^T e \tag{18}$$

where e is a vector of network errors and $\boldsymbol{J}$ is the Jacobian matrix that contains the first derivatives of the network errors. This matrix determination is computationally less expensive than the Hessian matrix. The new weight vector w_{n+1} can be adjusted as:

$$w_{n+1} = w_n - \left[\boldsymbol{J}^T \boldsymbol{J} + \mu \boldsymbol{I}\right]^{-1} \boldsymbol{J}^T e \tag{19}$$

The parameter μ is a scalar controlling the behaviour of the algorithm.

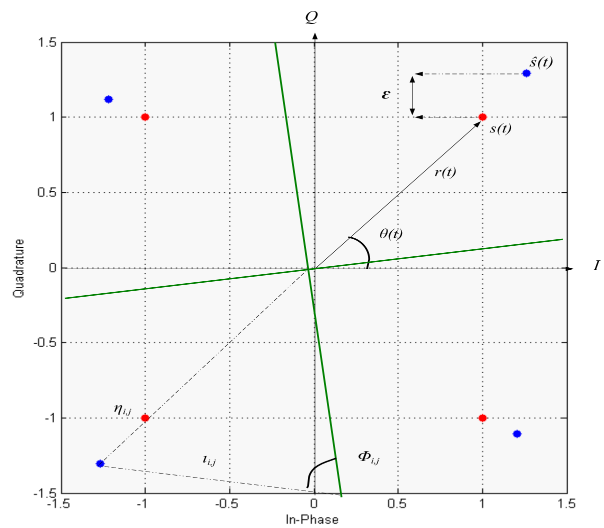

Fig. 3. Rectangular 4-QAM constellation and decision regions with NLN Receiver compensation without noise effect.

III. Performances in Terms of SER and EVM

In this section, we investigate the performance of MIMO-STBC systems over uncorrelated Rayleigh fading channels in the presence of HPA nonlinearity and NLN in terms of BER and EVM.

A. Derivation of the effective SNR Expression

In conventional MIMO-STBC systems, received signals from the NLN elements are combined at baseband. As the number of antenna elements increases, this receiver architecture becomes costly, especially for mobile devices [3]. However, if the signal combining takes place at the RF level, only one receive chain is required, which produces essentially the same output as with the conventional MRC receiver [11]. Hereafter, we consider the approach that combines signals from antenna elements at the RF level. The signal using the

 ISBN: 978-1-61208-236-3

NLN implementation scheme which enhances the cancellation of the distortion signal $\hat{\mathbf{s}}$ can be written as

$$\hat{s} = \hat{r}e^{j\hat{\theta}} \tag{20}$$

where $\hat{r}$ and $\hat{\theta}$ are the amplitude and the phase of $\hat{s}$, respectively. Let ε denotes the errors between the modulus of the input signal and the NLN output patterns. According to the equation (16) and using the central limit theorem, ε can be characterized by a gaussian distribution. For noislyless MIMO-STBC system, the variance of ε will be represented by [14]

$$\sigma_\varepsilon^2 = E\left\{|r_l - \hat{r}_l|^2\right\} = \left(r_l - \rho\sum_i u_i^m f(w_i^m\rho)\right)^2 \tag{21}$$

where ρ is the modulus of the NLN output and m denotes the coefficient of NLN identification. In this case ,the signal $\hat{s}$ can be rewritten as

$$\hat{s} = s + \boldsymbol{\varepsilon} \tag{22}$$

The error ε can be considered as a HPA nonlinearity results in modulus of the input s and output patterns $\hat{\mathbf{s}}$. An example illustrating such distortion is shown in Figure 3 where we present the constellation and the decision regions of a rectangular 4-QAM without and with HPA-NLN distortion.

We note that the error $\boldsymbol{\varepsilon}$ is uncorrelated with $\boldsymbol{N}$. In this case, the effective SNR at the output of the NLN can be expressed as:

$$\gamma^{STBC-NLN} = \frac{cE[A^2(r)]}{N_0 + \sigma_\varepsilon^2}\|\mathbf{H}\|_F^2 = \alpha\gamma^{STBC} \tag{23}$$

where $\|.\|_F$ denotes the Frobenius norm and γ^{STBC} is the effective SNR at the output of the distortion signal $\mathbf{Y}$:

$$\gamma^{STBC} = \frac{cE[A^2(r)]}{N_0}\|\mathbf{H}\|_F^2 \tag{24}$$

In this case, α can be expressed as:

$$\alpha = \frac{N_0}{N_0 + \sigma_\varepsilon^2} \tag{25}$$

Then, according to (25) into (23) , the effective SNR $\gamma^{STBC-NN}$ can be written as:

$$\gamma^{STBC-NLN} = \frac{cE[B^2(r)]}{N_0}\|\mathbf{H}\|_F^2 \tag{26}$$

where $E[B^2(r)] = \alpha E[A^2(r)] = P_s^{NLN}$ is the average power per symbol at the output of NLN.

B. SER evaluation

In this section, we evaluate the SER performance for the MIMO-STBC systems in the presence of both nonlinear HPA and NLN. Based on decision regions of the distorted version of the transmitted signal and constellation, the SER, can be expressed as a function of the instantaneous output SNR for arbitrary 2-D modulations, using Craig's method [15]

$$P_s(\gamma) = \sum_{i=1}^{M}\sum_{j=1}^{N_{s,i}} \frac{P_{s_i}}{2\pi}\int_0^{\eta_{i,j}} \exp\left[\frac{c_{i,j}\gamma\sin^{2\phi_{i,j}}}{\sin^2(\upsilon+\phi_{i,j})}\right] d\upsilon \tag{27}$$

where M is the number of symbols in the constellation, $N_{s,i}$ is the number of subregions for symbol s_i, P_{s_i} represents the a priory probability that symbol s_i is transmitted, γ is the output SNR of the MIMO-STBC system, and $c_{i,j} = l_{i,j}/\boldsymbol{P}_s^{NLN}$ is the scaling factor. Parameters $l_{i,j}$, $\eta_{i,j}$ and $\phi_{i,j}$ are related to the symbol s_i and the subregion j and is determined by the decision region geometry [3], [15] (see Figure 3).

The average SER using such decision region boundaries can be written as

$$P_s = \int_0^\infty P_s(\gamma)P_{\gamma^{STBC-NLN}}(\gamma)d\gamma \tag{28}$$

where $P_{\gamma^{STBC-NLN}}$ is the pdf of the output SNR for the MIMO-STBC system with NLN compensator under Rayleigh flat fading

$$P_{\gamma^{STBC-NLN}}(\gamma) = \tag{29}$$

$$\frac{2}{\Omega_{k,l}}\sqrt{\frac{\sigma_\Delta^2\gamma}{c\boldsymbol{P}_s^{NLN}}}\exp\left(-\frac{\sigma_\Delta^2\gamma}{c\boldsymbol{P}_s^{NLN}\Omega_{k,l}}\right) \tag{30}$$

where $\Omega_{k,l} = E[\lambda_{k,l}^2]$ represents the average fading power and $\lambda_{k,l}$ denotes the path gain. Substituting (27) and(29) into (28), the average SER can be rewritten as

$$P_s = \sum_{i=1}^{M}\sum_{j=1}^{N_{s,i}} \frac{P(s_i)}{2\pi}\int_0^{\eta_{i,j}} \boldsymbol{\Psi}_{\gamma^{STBC-NLN}}\left[\frac{c_{i,j}\sin^{2\phi_{i,j}}}{\sin^2(\upsilon+\phi_{i,j})}\right] d\upsilon \tag{31}$$

where $\boldsymbol{\Psi}_{\gamma^{STBC-NLN}}(j,\omega)$ is the characteristic function of $\gamma^{STBC-NLN}$ and is given by

$$\boldsymbol{\Psi}_{\gamma^{STBC-NLN}}(j,\omega) = \left\{1 - j\omega\frac{cG^2\boldsymbol{P}_s^{HPA}}{\sigma_\Delta^2}\right\}^m \tag{32}$$

Substituting (32) into (31) and making use of [3], [16], the average SER of MIMO-STBC over uncorrelated Rayleigh flat fading channels with NLN technique can be obtained by

$$\begin{aligned} P_s = \sum_{i=1}^{M}\sum_{j=1}^{N_{s,i}} \frac{P(s_i)}{2\pi} &\times \{\eta_{i,j} + \phi_{i,j} - \nu_{i,j} \\ &\times \left[\left(\frac{\pi}{2} + \arctan\lambda_{i,j}\right)\sum_{k=0}^{m\kappa-1}\binom{2k}{k}\right. \\ &\times \frac{1}{4^k\left(1+\varsigma_{i,j}\right)^k} + \sin\left(\arctan\lambda_{i,j}\right) \\ &\times \sum_{k=1}^{m\kappa-1}\sum_{l=1}^{k}\frac{T_{l,k}}{\left(1+\varsigma_{i,j}\right)^k} \\ &\left.\times\left(\cos\left(\arctan\lambda_{i,j}\right)\right)^{2(k-l)+1}\right]\Big\} \end{aligned} \tag{33}$$

where

$$\varsigma_{i,j} = c_{i,j}\left(c\boldsymbol{P}_s^{NLN}/\sigma_\Delta^2\right)\sin^2\phi_{i,j} \tag{34}$$

with

$$T_{l,k} = \binom{2k}{k} \Big/ \left[\binom{2(k-l)}{k-l} 4^l(2(k-l)+1)\right] \tag{35}$$

and $\nu_{i,j} = \sqrt{(\varsigma_{i,j}/(1+\varsigma_{i,j}))}sgn(\eta_{i,j}+\phi_{i,j})$ and $\lambda_{i,j} = -\varsigma_{i,j}\cot(\eta_{i,j}+\phi_{i,j})$

C. EVM degradation

The EVM is usually used as a parameter for evaluating the effects of imperfections in digital communication systems on the constellation diagram and is an effective method for calculating the system performance [17]. The EVM evaluation is based on the difference between an ideal transmitted constellation point $s(t)$ and the received symbol location $\hat{s}(t)$ at each symbol instant t. By definition [?], EVM is the root mean square (rms) value of the magnitudes of the error vectors Γ is expressed as

$$EVM_{rms} = \sqrt{\frac{1}{N_s}\sum_{t=1}^{N_s}|\Gamma|^2} \tag{36}$$

The residual error vector on sample s is obtained at each symbol instant and is defined as [17]

$$\Gamma = \frac{\hat{s}W^{-t} - C_0}{C_1} - s \tag{37}$$

where the complex constants C_0, C_1, and W compensate the constellation offset, constellation complex attenuation and the amplitude and offset phase rotation. The normalized EVM can be defined as the ratio of the rms EVM to the averaged symbol power [?] [18]

$$EVM_m = \frac{\sqrt{\frac{1}{N_s}\sum_{t=1}^{N_s}|\Gamma|^2}}{\sqrt{\frac{1}{N_s}\sum_{t=1}^{N_s}|s|^2}} = \frac{\sqrt{E\{|\Gamma|^2\}}}{E\{\sqrt{|\boldsymbol{s}|^2}\}} \tag{38}$$

The residual error vector Γ is obtained by

$$\Gamma = \hat{\boldsymbol{s}} - \boldsymbol{s} = Gc\|\boldsymbol{H}\|_F^2\boldsymbol{w} + \boldsymbol{v} + G\tilde{\boldsymbol{n}} = \Delta \tag{39}$$

Using the fact that the total noise sample and the interference term are uncorrelated, we can obtain the following expression

$$EVM_m = \frac{\sigma_\Delta^2}{\sqrt{\boldsymbol{P}_s}} \tag{40}$$

IV. SIMULATION RESULTS

To investigate the performance of the proposed NLN compensation in MIMO-STBC with HPA, a series of Monte Carlo simulations were carried out. The full-rate Alamouti code ($R_c = 1$, $c = 1$) is investigated. We have considered a MIMO system with 2 inputs and 2 outputs with 4-QAM modulation using 10^7 randomly generated symbol blocks. The memoryless selected nonlinear model for HPA is the TWTA one. The NLN (see Figure 2) neural network, is composed of two inputs, nine neurons in the hidden layer (with sigmoid activation function) and two linear neurons in the output layer. In the simulations, we define the input back-off (IBO) as:

$$IBO = 10\log_{10}(\frac{A_0^2}{P_{in}}) \tag{41}$$

where A_0^2 is the maximum output modulus and P_{in} is the average input power.

In order to identify the best SNR to create the learning data base, we have realised many data bases using various SNR, then we simulated the NLN to quarry out the SER obtained using MIMO-STBC system.

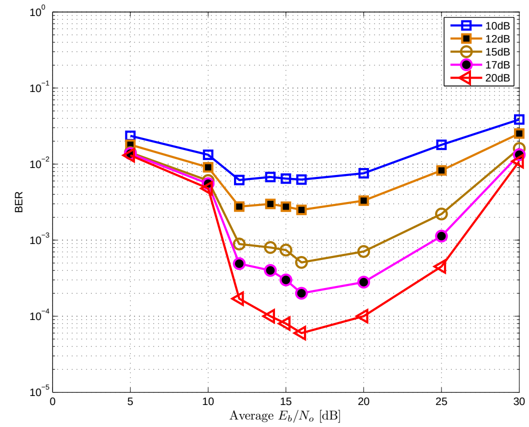

Fig. 4. SER over MIMO-STBC system with NLN correction (Fixed SNR simulation for each curve).

Figure 4 shows the SER performs versus the SNR used in the learning phase with different SNR used in generalization phase. We note from these results that in all cases, the learning data base with SNR around 16 dB offers the best performs. For our simulations, we have used a learning data base with SNR equal 16 dB.

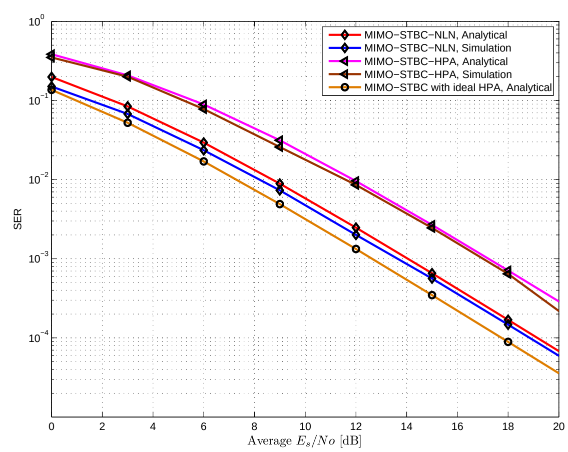

Fig. 5. The SER of signal transmission over MIMO-STBC system.

Figure 5 shows the average SER performances of the considered system for three cases i) MIMO-STBC with ideal HPA which serves as a benchmark. ii) MIMO-STBC-NLN iii) MIMO-STB-HPA without compensation. We show that analytical and simulation results are in perfect match. We note that the NLN is able to improve the system performance.

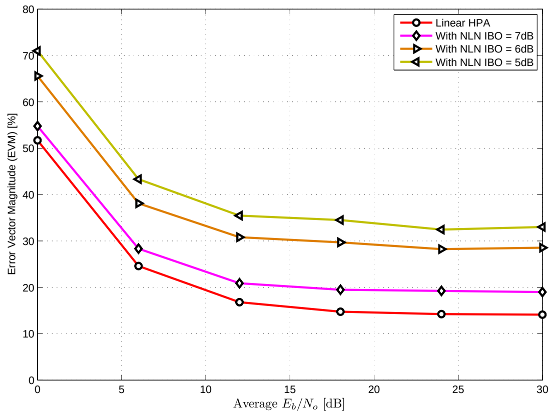

Fig. 6. EVM_m as a function of SNR with the IBO as parameter.

Figure 6 illustrates the EVM of Equation (40) versus SNR and selected IBO values. It indicates that SNR imposes a great impact on the EVM performance when the IBO varies.

V. Conclusion

In this paper, the effects of nonlinear HPA on the performance of the MIMO-STBC system were evaluated when it is operated under Rayleigh fading channel. It was shown that the NLN technique implemented at the receiver is able to compensate the nonlinear behaviour caused by the power amplifier. The simulation results showed that, in the presence of the proposed NLN decreased the used SNR to 14 dB at SEP to 10^{-4} which is an improvement of more than 3 dB compared to HPA without compensation. The system performance was analyzed in terms of effective SNR expression, average SER and EVM. Theoretical results show a close matching with those obtained by simulations for the 4-QAM MIMO-STBC systems.

References

[1] R. Z. R. Bouallegue and D. Roviras, "Adaptive Pre-distortions based on Neural Networks associated with Levenberg-Marquardt algorithm for Satellite Down Links," *EURASIP Journal on Wireless Communications and Networking*, vol. 2008, pp. 1–8, 2008.

[2] A. J. Goldsmith, S. A. Jafar, N. Jindal, and S. Vishwanath, "Capacity Limits of MIMO Channels," *IEEE Journal on Selected Areas in Communication*, vol. 21, no. 5, pp. 684–702, June 2003.

[3] Q. Jian and S.Aissa, "Analysis and Compensation of Power Amplifier Nonlinearity in MIMO transmit Diversity Systems," *IEEE Transactions on Vehicular Technology*, vol. 59, pp. 2921–2931, July 2010.

[4] F. H. Gregorio, "Analysis and Compensation of Nonlinear Power Amplifier effects in Multi-antenna OFDM Systems," Ph.D. dissertation, Helsinki Univ. Technol, Nov 2007.

[5] A. A. M. Saleh, "Frequency-independent and Frequency-dependent Nonlinear Models of TWT Amplifiers," *IEEE Transaction on Communication*, vol. 29, pp. 1715–1720, 1981.

[6] R. Z. R. Bouallegue and D. Roviras, "Crossover Neural Network Predistorter for the Compensation of Crosstalk and Nonlinearity in MIMO OFDM Systems," in *IEEE 21st International Symposium on Personal Indoor and Mobile Radio Communications Information Sciences System*, 2010.

[7] A. Al-Hinai and M. Ibnkahla, "Neural Network Nonlinear MIMO Channel Identification and Receiver Design," in *IEEE International Conference on Communications, ICC '08*, 2008, pp. 835 –839.

[8] Q. Jian and S. Aissa, "Impact of hpa Nonlinearity on MIMO Systems With Quantized Equal Gain Transmission," in *20th IEEE International Symposium on Personal, Indoor and Mobile Radio Communications, PIMRC'09*, 2009, pp. 2891 – 2895.

[9] G. Santella and F. Mazzenga, "A Hybrid Analytical-Simulation Procedure for Performance Evaluation in M-QAM-OFDM Schemes in Presence of Nonlinear Distortions," *IEEE Trans. Veh. Technol.*, vol. 47, pp. 142–151, Feb 1998.

[10] H. E. Rowe, "Memoryless Nonlinearities with Gaussian Inputs: Elementary Results,," *Bell Syst. Tech. J.*, vol. 61, pp. 1519–1525, Sept 1982.

[11] J. Qi and S. Aissa, "On The Effect of Power Amplifier Nonlinearity on MIMO Transmit Diversity Systems," in *Proc. IEEE ICC*, Dresden, Germany, 2009.

[12] D. Dardari and V. T. A. Vaccari, "A Theoretical Characterization of Nonlinear Distortion Effects in OFDM Systems," *IEEE Trans. Commun.*, vol. 48, pp. 1755–1764, 2000.

[13] M. Ibnkahla, "Applications of Neural Networks to Digital Communications Survey," *Signal Processing*, vol. 80, no. 7, pp. 1185–1215, 2000.

[14] D. R. H. Abdulkader, F. Langlet and F. Castanie, "Natural gradient algorithm for neural networks applied to non-linear high power amplifiers," *Int. J. Adapt. Control Signal Process*, vol. 2, no. 16, pp. 557–576, 2002.

[15] J. W. Craig, "A New, Simple and Exact Result for Calculating the Probability of Error for Two Dimensional Signal Constellations," in *Proc. IEEE MILCOM*, 1991.

[16] M. S. Alouini and M. K. Simon, "An MGF Based Performance Analysis of Generalized Selection Combining Over Rayleigh Fading Channels," *IEEE Trans. Commun*, vol. 48, pp. 401–415, 2000.

[17] H. Zareian and V. T. Vakili, "Analytical EVM, BER, and TD Performances of the OFDM Systems in the Presence of Jointly Nonlinear Distortion and IQ Imbalance," *Springer-Verlag*, vol. 64, pp. 753–762, 2009.

[18] A. Georgiadis, "Gain, Phase Imbalance, and Phase Noise Effects on Error Vector Magnitude," *IEEE Trans Veh Tech*, vol. 2, pp. 443–449, 2004.